

Cite this: DOI: 00.0000/xxxxxxxxxx

Electronic Supplementary Information for: Electron and ion spectroscopy of the cyclo-alanine-alanine dipeptide

Jacopo Chiarinelli,^a Darío Barreiro-Lage,^{*b} Paola Bolognesi,^{*a} Robert Richter,^c Henning Zettergren,^d Mark H. Stockett,^d Sergio Díaz-Tendero,^{b,e,f} and Lorenzo Avaldi^a

1 The ion-neutral coincidence experiment: simulation

The fragmentation paths producing the ‘traces’ in the ion-neutral coincidence experiments cannot be directly identified by looking at the 2D coincidence map, Fig.3 (main paper). The unknown variation of detection efficiency of the MCP for different kinetic energies of the neutral fragments affects the intensity of the ‘traces’, that faint out at the longest TOF_2 . Thus a relevant fraction of each ‘trace’ cannot be visualised. Indeed, the ‘trace’ of the $P_{ion} \rightarrow D_{ion} + N_{frag}$ process converges asymptotically to the TOF of the (D_{ion}). These long flight times correspond to early fragmentations, i.e. events producing neutral fragment with low ion kinetic energies. The limit of convergence of a ‘trace’ may therefore be not visible due to poor detection efficiency of the MCP for low kinetic energy neutral fragments, and/or extend beyond the 9 μs time window chosen for the present measurements.

The line-shape of each ‘trace’ in the 2D coincidence map is directly connected to i) the mass and charge of each particle, P_{ion} , D_{ion} and N_{frag} , involved in the fragmentation, ii) the time interval between ionisation and fragmentation, t_f , and iii) the geometry of the experimental set-up and the electric field experienced by the particles. For these reasons, a computer simulation of the trajectory of the charged/neutral fragments in the set-up is a necessary tool to provide information about the correlated particles in the $P_{ion} \rightarrow D_{ion} + N_{frag}$ process. To this purpose, we have developed a simulation procedure using the Igor Pro¹ software where the detailed description of the electric field active in the set-up is imported from the ion optics simulation software SIMION². The path and flight time of each particle is simulated using the ‘mid-point’ numerical method:

$$a_i = \frac{q_i E(x_i)}{m_i} \quad (1)$$

$$v_{i+1} = v_i + a_i \Delta t \quad (2)$$

$$x_{i+1} = x_i + \frac{1}{2}(v_i + v_{i+1})\Delta t \quad (3)$$

where a , v , x , q and m are the acceleration, velocity, position, charge and mass of the particle and $E(x)$ the electric field at the position x . The indexes i and $i + 1$ identify two subsequent steps of the iteration separated by a time-step $\Delta t = 0.5$ ns.

The electric field E has a cylindrical symmetry about the axis (labelled x-axis) of the time-of-flight spectrometer. The relevant parameter here is the flight time of the particles along the x-axis. For this reason in the simulation we have taken into account only the x component of all the vectorial quantities of the simulation (position, velocity and acceleration of the particles and electric field).

To begin the simulation defined by equations 1-3, the initial values x_0 and v_0 of the ions have to be defined. The starting positions of the simulation, corresponding to the ionisation region, are obtained by a Gaussian probability distribution G centered in \bar{x} , the middle point between the extractor and the repeller of the Time-of-flight spectrometer, with a standard deviation $d = 1$ mm :

$$P(x_0) = G(\bar{x}, d) \quad (4)$$

^a Institute of Structure of Matter-CNR (ISM-CNR), 00015 Monterotondo, Italy.

^b Departamento de Química, Universidad Autónoma de Madrid, 28049 Madrid, Spain.

^c Elettra Sincrotrone Trieste, 34149 Basovizza, Trieste, Italy.

^d Department of Physics, Stockholm University, Se-10691 Stockholm, Sweden.

^e Condensed Matter Physics Center (IFIMAC), Universidad Autónoma de Madrid, 28049 Madrid, Spain

^f Institute for Advanced Research in Chemical Science (IAdChem), Universidad Autónoma de Madrid, 28049 Madrid, Spain.

* Email: paola.bolognesi@cnr.it, dario.barreiro@uam.es

The initial velocity is isotropically distributed and its intensity on the x-axis, v_0 , is obtained by a Gaussian distribution centered at zero with a standard deviation equal to $\sqrt{k_B T/m}$:

$$P(v_0) = G_{(0, \sqrt{k_B T/m_P})} \quad (5)$$

where m_P is the mass of the parent ion, k_B the Boltzmann constant and $T = 85^\circ\text{C}$ the evaporation temperature. The time of the fragmentation, t_f , is obtained by an exponential distribution probability:

$$P(t_f) = \int_{t_f}^{t_f+dt} k e^{-kt} dt \quad (6)$$

where k is the decay rate and indicates the mean number of events in the unit of time. The value of k may be obtained experimentally by an analysis of the intensity changes along the ‘trace’. However, this analysis necessarily requires the knowledge of the MCP detection efficiency for neutral fragments of different kinetic energies. This being unknown, here we cannot estimate the decay rate, but only simulate the traces to correlate the different D_{ion}, N_{frag} pairs produced in the $P_{ion} \rightarrow D_{ion} + N_{frag}$ process.

For each ‘trace’ of Fig.3, 20000 fragmentation events have been simulated. For all ‘traces’, an arbitrary k value of $2 \cdot 10^5 \text{ s}^{-1}$ has been used. This value does not necessarily correspond to a decay rate, but it is sufficiently large to produce a reasonable number of fragmentation events along the entire t_f range experimentally observable, i. e. about (0 – 1000) ns according to the results of the simulations presented in Section 2 of the main article, and to clearly visualise the ‘trace’. The velocities on the x-axis v_D and v_N of the daughter ion and the neutral fragment, immediately after the fragmentation, are calculated using the following equations derived from the momentum and energy conservation laws:

$$v_D = v_P + v'_D = v_P + \cos(\alpha) \sqrt{\frac{2m_N |KER|}{3(m_D^2 + m_D m_N)}} \quad (7)$$

$$v_N = v_P - v'_D m_D / m_N \quad (8)$$

$$P(\alpha) = U_{(0, 2\pi)} \quad (9)$$

$$P(KER) = G_{(0, \varepsilon)} \quad (10)$$

where v_P is the velocity of the parent ion immediately before the fragmentation while m_D and m_N are the masses of the daughter ion and neutral fragment, respectively. α is the angle between the isotropically distributed axis of the fragmentation and the x-axis and is obtained by a uniform probability distribution in the range (0, 2π) (equation 9). KER is the kinetic energy release of the fragmentation and is obtained by a Gaussian distribution centered at zero with a standard deviation equal to ε (equation 10).

The effect of the parameter KER in the simulation of a ‘trace’ is to increase the time spread as shown in Figure 1. The use of different KER values in the simulation of a ‘trace’ does not preclude the identification the fragmentation path. For these reasons, a value of $\varepsilon = 0$ has been used for all the simulated fragmentation events.

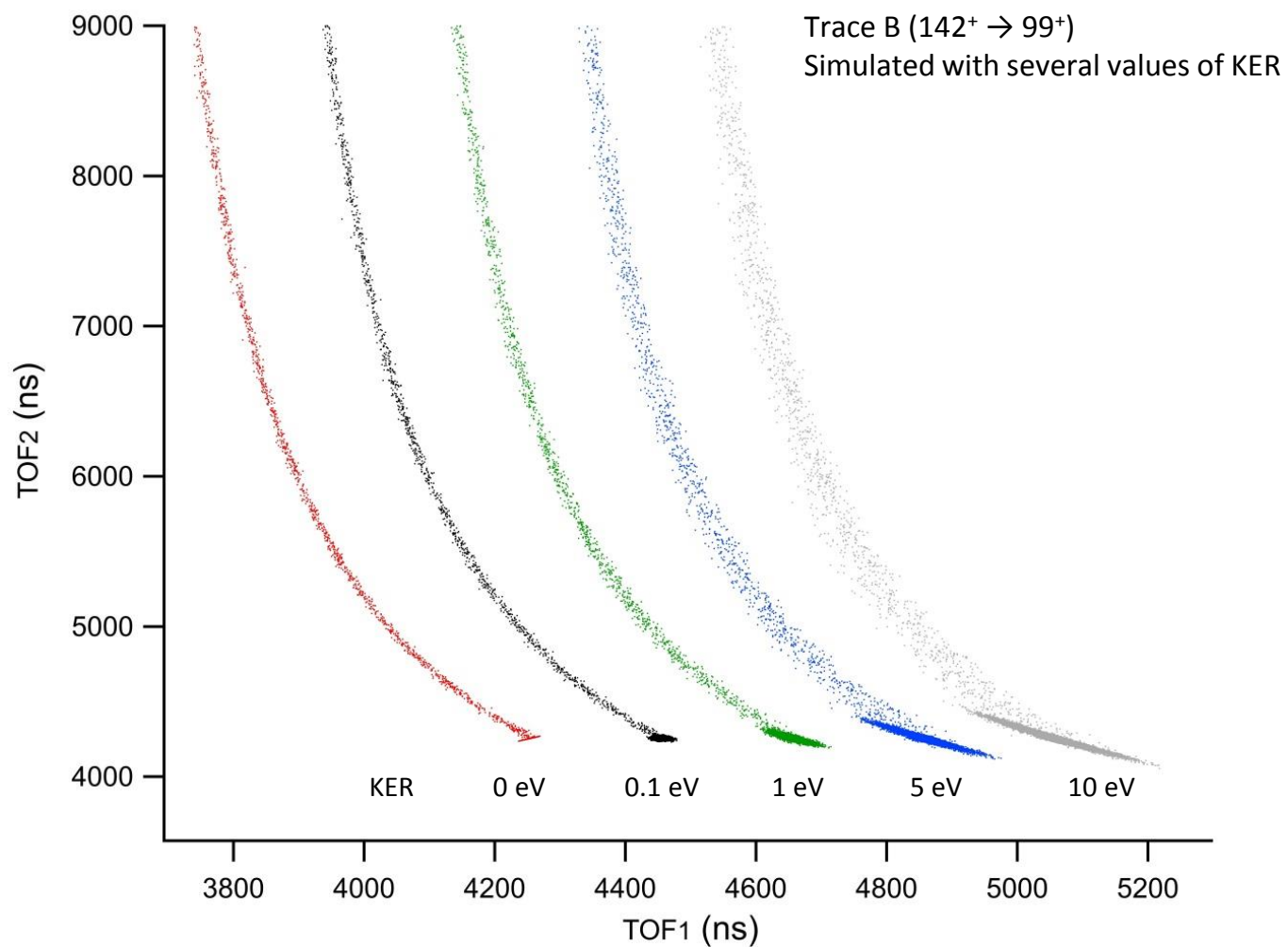


Figure 1 Simulation of the fragmentation represented by trace B, $142^+ \rightarrow 99^+$ in Fig.3 (main text) and Fig.2[†] in ESI performed with several values of the KER in the range 0 – 10 eV. The trace for KER=0 is reported in the original position while the other traces are shifted by 200ns on the TOF_1 axis.

2 The ion-neutral coincidence maps at several photon energies

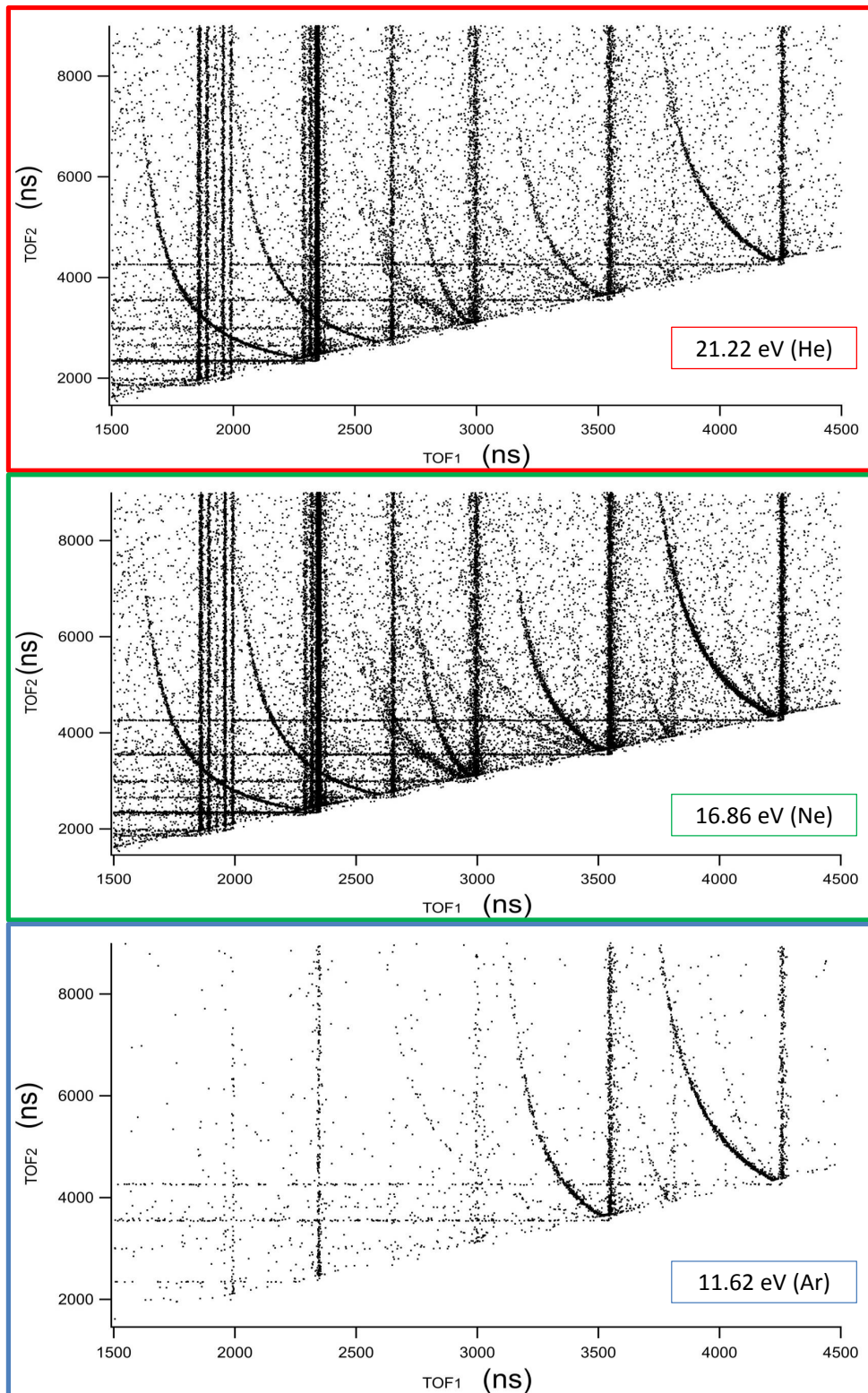


Figure 2 The ion-neutral coincidence experiments have been performed at three different photon energies, namely 21.22, 16.85 and 11.62 eV corresponding to main emission lines of the discharge lamp operated with He, Ne and Ar gases, respectively.

3 cAA conformers and molecular orbitals

Figure 3 shows the two most stable conformers calculated for the cAA diketopiperazine. An initial guess for structures were sampled using the GFN2-xTB Hamiltonian as implemented in the CREST tool³. Within an energy window of 300 kcal/mol only three different conformers were obtained which were reduced to two after energy relaxation at higher level of theory DFT-B3LYP/6-311++G(d,p), both shown in Fig. 3.

Six first occupied molecular orbitals for the most stable conformer of cAA, calculated with Hartree-Fock and the 6-311G(d,p) basis set, are shown in Fig. 4.

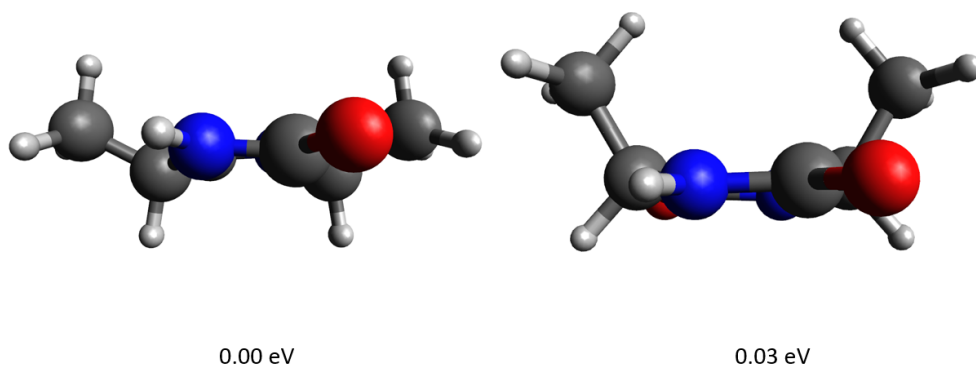


Figure 3 Lowest energy conformers of cAA calculated at the DFT-B3LYP/6-311++g(d,p) level of theory.

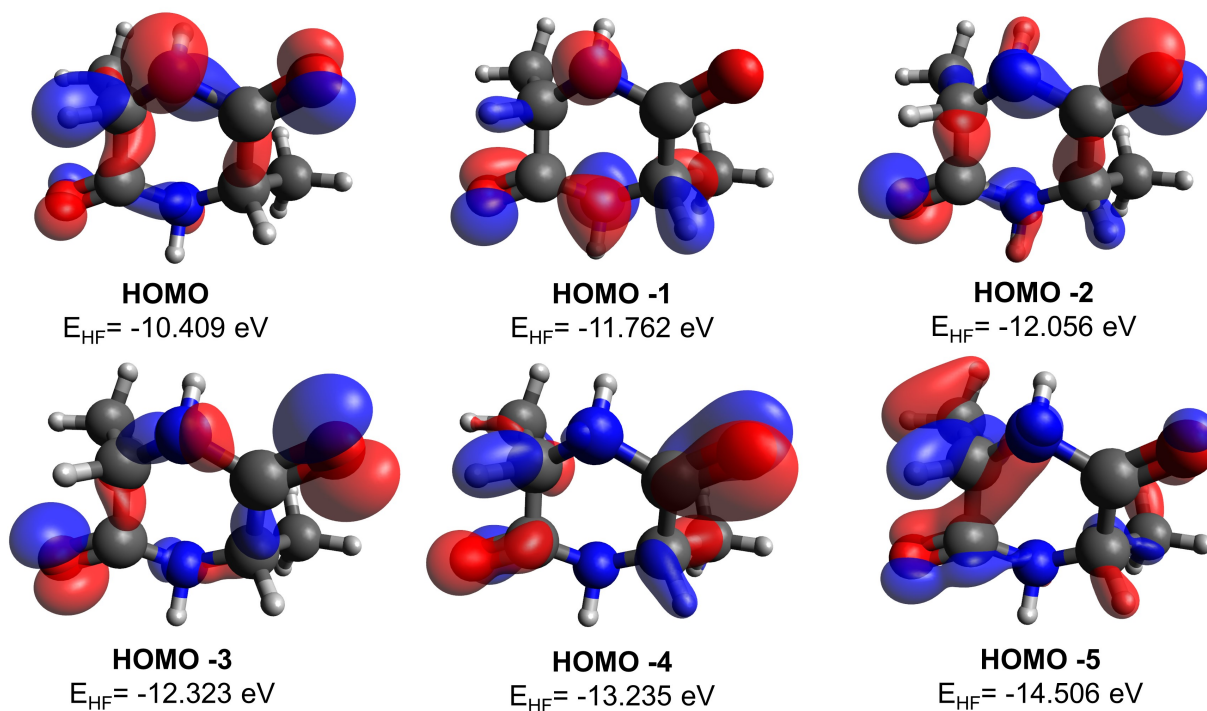


Figure 4 The cAA Molecular orbitals calculated at the HF/6-311G(d,p) level of theory over the geometry of the most stable neutral conformer optimized at the DFT-B3LYP/6-311++G(d,p) level of theory.

4 Mechanism for the $99^+ \rightarrow 58^+$ fragmentation channel

Charged fragment 58^+ is almost invisible in the PEPICO experiments, however, the ion-neutral coincidence experiment showed an interesting trace representing the fragmentation path of fragment 99^+ towards 58^+ ($99^+ \rightarrow 58^+$). This mechanism, starting from a very low-in-energy minimum (9.00 eV) after the direct loss of HNC0 (channel blue in Fig. 6 of the main paper), is a complex mechanism that involves several hydrogen transfers and the break-up of the peptidic NH–CO bond. Quantum chemistry calculations were performed to obtain the energy barriers involved in this process and are shown in Fig. 5. Channels blue and orange arrive to the same minimum (at 9.47 eV) but with different order in the two hydrogen transfers. From here, two different transition states can take place, being the higher-in-energy the one arriving to the charged 58^+ fragment, while the lower-in-energy implies the formation of fragment 42^+ .

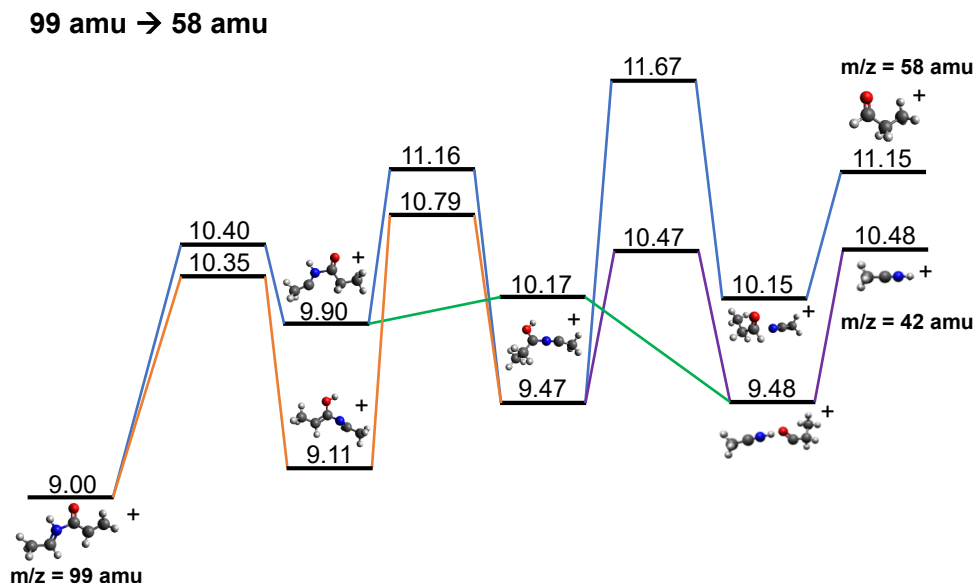


Figure 5 Potential Energy Surface exploration for the channel from 99^+ to 58^+ . All points are referred to the neutral cAA most stable conformer and were calculated at a B3LYP/6-311G(d,p) level of theory.

Notes and references

- 1 Wavemetrics Inc., *Igor Pro*, <https://www.wavemetrics.com>.
- 2 Scientific Instrument Services, Inc., *SIMION*, <https://www.simion.com>.
- 3 P. Pracht, F. Bohle and S. Grimme, *Phys. Chem. Chem. Phys.*, 2020, **22**, 7169–7192.